Atlantic overturning circulation and Agulhas leakage influences on southeast Atlantic upper ocean hydrography during marine isotope stage 11

Alexander J. Dickson,[1,2] Melanie J. Leng,[3,4] Mark A. Maslin,[1] Hilary J. Sloane,[3] Joanne Green,[3] James A. Bendle,[5] Erin L. McClymont,[6] and Richard D. Pancost[7]

Received 29 July 2009; revised 17 November 2009; accepted 24 February 2010; published 7 August 2010.

[1] Climate dynamics during the marine isotope stage (MIS) 11 interglacial may provide information about how the climate system will evolve under the conditions of low-amplitude orbital forcing that are also found during the late Holocene. New stable isotope and alkenone data are presented from southeast Atlantic Ocean Drilling Program Site 1085, providing detailed information on interglacial climate evolution and the impacts of Atlantic meridional overturning circulation (MOC) and Agulhas leakage on the regional upper ocean hydrography. The data suggest that although warm surface ocean conditions were maintained at approximate Holocene levels for 40,000 years during MIS 11, subsurface temperature and salinity recorded by deeper-dwelling planktonic foraminifera species were maintained at their highest values for only 7000–8000 years. Surface water temperature and salinity data suggest that the interocean exchange of warm, salty waters into the southeast Atlantic Ocean was directly related to changes in the activity of the MOC during the study interval. Specifically, transient regional warming events during periods of weakened overturning circulation may have been amplified by the continuous interocean exchange of warm, salty Indian Ocean waters that primed the MOC for abrupt resumptions into a vigorous mode of operation. Conversely, a peak in interocean exchange at the end of the MIS 11 interglacial optimum may reflect enhanced trade wind forcing of surface waters whose export to the North Atlantic Ocean could have contributed to renewed ice sheet buildup during the MIS 11 to 10 glacial inception.

Citation: Dickson, A. J., M. J. Leng, M. A. Maslin, H. J. Sloane, J. Green, J. A. Bendle, E. L. McClymont, and R. D. Pancost (2010), Atlantic overturning circulation and Agulhas leakage influences on southeast Atlantic upper ocean hydrography during marine isotope stage 11, *Paleoceanography*, *25*, PA3208, doi:10.1029/2009PA001830.

1. Introduction

[2] Over timescales of thousands to hundreds of thousands of years, the climate system is forced principally by changes in the amount and distribution of solar radiation received across the surface of the Earth. These insolation changes are amplified or repressed by feedback processes operating within the oceans, atmosphere, cryosphere, and biosphere, giving rise to nonuniform climate changes in different regions and abrupt climate events that cannot be explained with reference to orbital forcing. One way of understanding how climate feedbacks could operate in the present day is to examine past periods of warm climate, such as the late Quaternary interglacials. Of the five warm interglacials that have occurred since a sharp change in the amplitude of glacial-interglacial cycles during the middle Brunhes transition [*EPICA community members*, 2004], marine isotope stage (MIS) 11 has received close attention because of a near-circular Earth orbit, which produced a low-amplitude precession cycle similar to the present day [*Berger and Loutre*, 2002; *Loutre and Berger*, 2003].

[3] One of the most widely studied players in global climate change is the meridional overturning circulation (MOC), which directly affects regional distributions of oceanic heat and atmospheric moisture and indirectly controls atmospheric greenhouse gas concentrations by affecting the distribution of alkalinity in the global ocean. The southeast Atlantic Ocean is an important region for the MOC as a route through which surface waters are transported on their return journey toward the North Atlantic Ocean. Surface waters enter the southeast Atlantic Ocean from the Indian Ocean via the shedding of warm water "rings" and the advection of warm water filaments within the Agulhas Retroflection around the tip of southern Africa [*Gordon et al.*, 1992; *Lutjeharms*, 1996, 2006]. Recent work has suggested that a

[1]Environmental Change Research Centre, Department of Geography, University College London, London, UK.
[2]Now at Department of Earth and Environmental Sciences, Open University, Milton Keynes, UK.
[3]NERC Isotope Geosciences Laboratory, British Geological Survey, Keyworth, Nottingham, UK.
[4]School of Geography, University of Nottingham, Nottingham, UK.
[5]Glasgow Molecular Organic Geochemical Laboratory, Department of Geographical and Earth Science, University of Glasgow, Glasgow, UK.
[6]School of Geography, Politics, and Sociology, University of Newcastle upon Tyne, Newcastle upon Tyne, UK.
[7]Organic Geochemistry Unit, Bristol Biogeochemistry Research Centre, School of Chemistry, University of Bristol, Bristol, UK.

0883-8305/10/2009PA001830

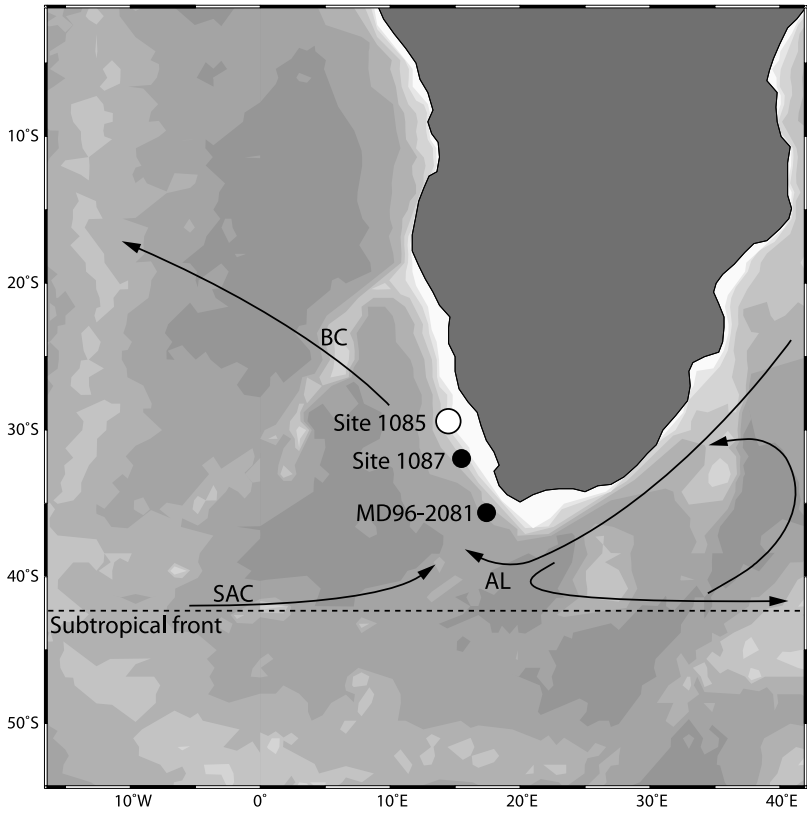

Figure 1. Location of studied core site (white circle) and core sites mentioned in the text (black circles). Solid lines represent the flow paths of the main regional surface and near-surface waters. AL, Agulhas leakage; SAC, South Atlantic Current; BC, Benguela Current. Dashed line represents the approximate modern latitude of the subtropical front.

larger mass transport of Agulhas waters into the South Atlantic Ocean increases the salinity of the return limb of the MOC, thereby contributing to warm (Northern Hemisphere) climates through strong positive MOC feedbacks [*Gordon*, 1996; *Flores et al.*, 1999; *Giraudeau et al.*, 2001; *Rau et al.*, 2002; *Knorr and Lohmann*, 2003; *Peeters et al.*, 2004; *Cortese et al.*, 2007; *Biastoch et al.*, 2008; G. Martinez-Mendez et al., A 345,000 year record of heat and salt transports in the Agulhas corridor south of Africa, submitted to *Paleoceanography*, 2009]. Conversely, a sluggish MOC is thought to produce regional surface and subsurface warming in the southeast Atlantic Ocean as the northward advection of subtropical Indian Ocean water masses accumulating in the South Atlantic Ocean is weakened [e.g., *Wefer et al.*, 1996; *Rühlemann et al.*, 1999, 2004; *Kim et al.*, 2002; *Chang et al.*, 2008].

[4] Our understanding of paleoceanographic changes during MIS 11 has been improved with several high-resolution surface water paleoceanographic reconstructions in the North Atlantic [*Oppo et al.*, 1998; *McManus et al.*, 2003; *Billups et al.*, 2004; *de Abreu et al.*, 2005; *Martrat et al.*, 2007; *Kandiano and Bauch*, 2007] and Southern oceans [*Hodell et al.*, 2003; *Kunz-Pirrung et al.*, 2002]. However, few high-resolution (submillennial to centennial) scale records exist outside of these regions. This study presents a new submillennial-scale resolution surface water data set of the MIS 11 interglacial from the southeast Atlantic Ocean. These data are used to investigate how the upper water column hydrography (vertical structure, temperature, salinity) evolved throughout this period, with implications for the regional evolution of interglacial paleoceanographic conditions and the role of the Agulhas leakage on MOC variability over glacial-interglacial and millennial timescales.

2. Methods

2.1. Study Site and Sampling

[5] Ocean Drilling Program (ODP) Site 1085 (29.2°S, 13.6°E, 1713 m) is located on the southwest African continental slope in the path of the northward flowing Benguela Current (Figure 1). Although seasonally affected by nutrient-rich filaments of upwelled water [*Lutjeharms et al.*, 1991; *Romero et al.*, 2002], upper ocean hydrography over Site 1085 is not characteristic of an upwelling site, with the development of a strong thermocline at ~90 m depth during austral summer, when coastal upwelling at the nearby Namaqua upwelling cell is at a maximum. Conversely, the thermocline becomes weaker during austral winter when coastal upwelling is weaker [*Shannon and Nelson*, 1996; *Locarnini et al.*, 2006]. The annual sea surface temperature range is 4.5°C, reaching a maximum of 20°C in January [*Locarnini et al.*, 2006].

[6] Sampling of ODP 1085B was guided by low-resolution benthic $\delta^{18}O$ measurements covering most of the middle to late Quaternary [*Westerhold*, 2003]. One centimeter thick samples were taken at 2 cm intervals from core 2H, between 11.00 and 17.50 m below seafloor (mbsf). Each sample was freeze-dried and split for foraminifera, bulk sediment, and biomarker analyses.

2.2. Oxygen Isotopes

[7] Using ultrapure (18.2 MΩ) deionized water, 5–10 g of material were wet sieved over a 63 μm mesh sieve. The coarse and fine residues were oven dried at 40°C and stored until further use. Oxygen isotopes were measured on two species of planktonic foraminifera, *Neogloboquadrina incompta* [*Darling et al.*, 2006] and *Globigerinoides truncatulinoides* (dextral), and on bulk fine sediment dominated by fine coccolith carbonates (<63 μm). *G. truncatulinoides* (dextral) is a deep-dwelling nonsymbiotic species that has been used as an indicator of subthermocline water mass changes [e.g., *de Vargas et al.*, 2001; *Cléroux et al.*, 2007], and *N. incompta* is a nonsymbiotic species that calcifies at subsurface depths in response to the availability of sinking food sources [e.g., *Fairbanks et al.*, 1980; *Ortiz et al.*, 1995; *Darling et al.*, 2006]. To limit the effects of ontogeny, 30–40 individuals of each foraminifera species were picked from the 250–300 μm size fraction [*Lončarić et al.*, 2006]. Samples were rinsed in 18.2 MΩ water and gently crushed and homogenized using a pestle and mortar. Sixty to eighty micrograms of calcite was weighed into small glass vials and reacted at 90°C in a common acid bath attached to a VG Optima dual-inlet mass spectrometer. Bulk fine sediment (<63 μm) oxygen isotopes were measured on 10 mg carbonate equivalent samples, which were ground in agate and reacted with anhydrous phosphoric acid under vacuum overnight at a constant 25°C. The CO_2 liberated was separated and collected for analysis. The $\delta^{18}O$ values are expressed relative to the Vienna Pee Dee belemnite (VPDB) scale by reference to an internal laboratory working standard Keyworth carbonate marble (KCM) calibrated against NBS 19. Reproducibility was estimated from repeat measurements of KCM and was <0.1‰.

2.3. Alkenone $U^{K'}_{37}$

[8] Alkenones were extracted from ground bulk sediment and measured for the intervals between 11.04–13.91 and 16.96–17.40 mbsf using the methods described by *Dickson et al.* [2009]. The $U^{K'}_{37}$ values [*Prahl and Wakeham*, 1987] were converted to estimated mean annual sea surface temperatures [*Müller and Fischer*, 2003] using the global core top calibration of *Conte et al.* [2006] which produces near-identical values for the study region as the global calibration of *Müller et al.* [1998] but has a more extensive modern core top database.

2.4. Calculating $\delta^{18}O_w$

[9] The $\delta^{18}O$ composition of foraminifera calcite (δ_c) is mainly controlled by changes in the $\delta^{18}O$ composition of the source water (δ_w) and the temperature-dependent fractionation of $\delta^{18}O$ during calcification (mediated by biogeochemical vital effects). If global seawater $\delta^{18}O_w$ and the magnitude of the temperature-dependent fractionation are known, then the residual isotopic effect linked to local seawater salinity changes can be estimated. This principle has been used to calculate residual upper ocean $\delta^{18}O_w$ from measurements of fine carbonate $\delta^{18}O$. The magnitude of the temperature-driven $\delta^{18}O$ fractionation (here labeled δ_T) has been estimated using $U^{K'}_{37}$ sea surface temperature (SST) to reflect coccolithophore calcification temperatures [e.g., *Beltran et al.*, 2007] using the empirical paleotemperature equation, $\delta_T = 4.34 - 0.2 \times T$, derived by *Dudley et al.* [1986] for "small" coccolithophores (including *G. oceanica*, *E. huxleyei*, and *Crenoolithus* spp.). Using the paleotemperature equation given by *Ziveri et al.* [2003] gives values that are systematically offset by ~0.25‰. The global component of seawater $\delta^{18}O$ linked to ice volume change has been calculated from the Red Sea sea level data of *Rohling et al.* [2009] using a scaling of 0.01‰/m (details in the auxiliary material).[1] For consistency with existing studies [*Bemis et al.*, 1998; *Ziveri et al.*, 2003], calculated values of $\delta^{18}O_w$ were converted from VPDB to Vienna SMOW (VSMOW) by adding 0.27‰. Sea surface salinity was not estimated from residual $\delta^{18}O_w$ because of the large errors associated with these calculations [e.g., *Rohling*, 2000]. Here the error associated with the $\delta^{18}O_w$ calculation is estimated as ±0.3‰ (1σ) on the basis of a propagation of the SST error (±1.7°C), $\delta^{18}O$ measurement (±0.1‰), the scatter in *Dudley et al.*'s [1986] paleotemperature equation, and error associated with the measurement and calculation of the Red Sea sea level curve (±0.12‰).

2.5. Age Model

[10] All data in Figures 4 and 5 have been plotted on the LR04 age model [*Lisiecki and Raymo*, 2005] following correlation of the benthic $\delta^{18}O$ record from Site 1085 to the LR04 benthic stack [*Dickson et al.*, 2008]. The data cover the period between approximately 335 and 475 ka at a mean resolution of 435 years between samples.

3. Validation of Proxy Data

3.1. Foraminifera Calcification Depth Habitats

[11] Interpreting the $\delta^{18}O$ signal of planktonic foraminifera can be complicated by several effects such as seawater pH changes induced by algal symbionts in spinose species [*Spero et al.*, 1997] and by vertical migration and the production of gametogenic calcite in mature individuals [*Mulitza et al.*, 2003; *McKenna and Prell*, 2004]. The influence of local pH variability and ontogeny on the $\delta^{18}O$ records of *N. incompta* and *G. truncatulinoides* (dextral) (Figure 2) is likely to be small because neither species supports algal symbionts and because measurements have been made on a small (50 μm) size range.

[12] Calcification depths have been calculated for each foraminifera species by comparing core top $\delta^{18}O$ values from nearby multicore GeoB1720-2 to profiles of predicted $\delta^{18}O_c$ for the regional water column. These profiles have been estimated from atlas salinity values [*Locarnini et al.*, 2006]

[1] Auxiliary materials are available in the HTML. doi:10.1029/2009PA001830.

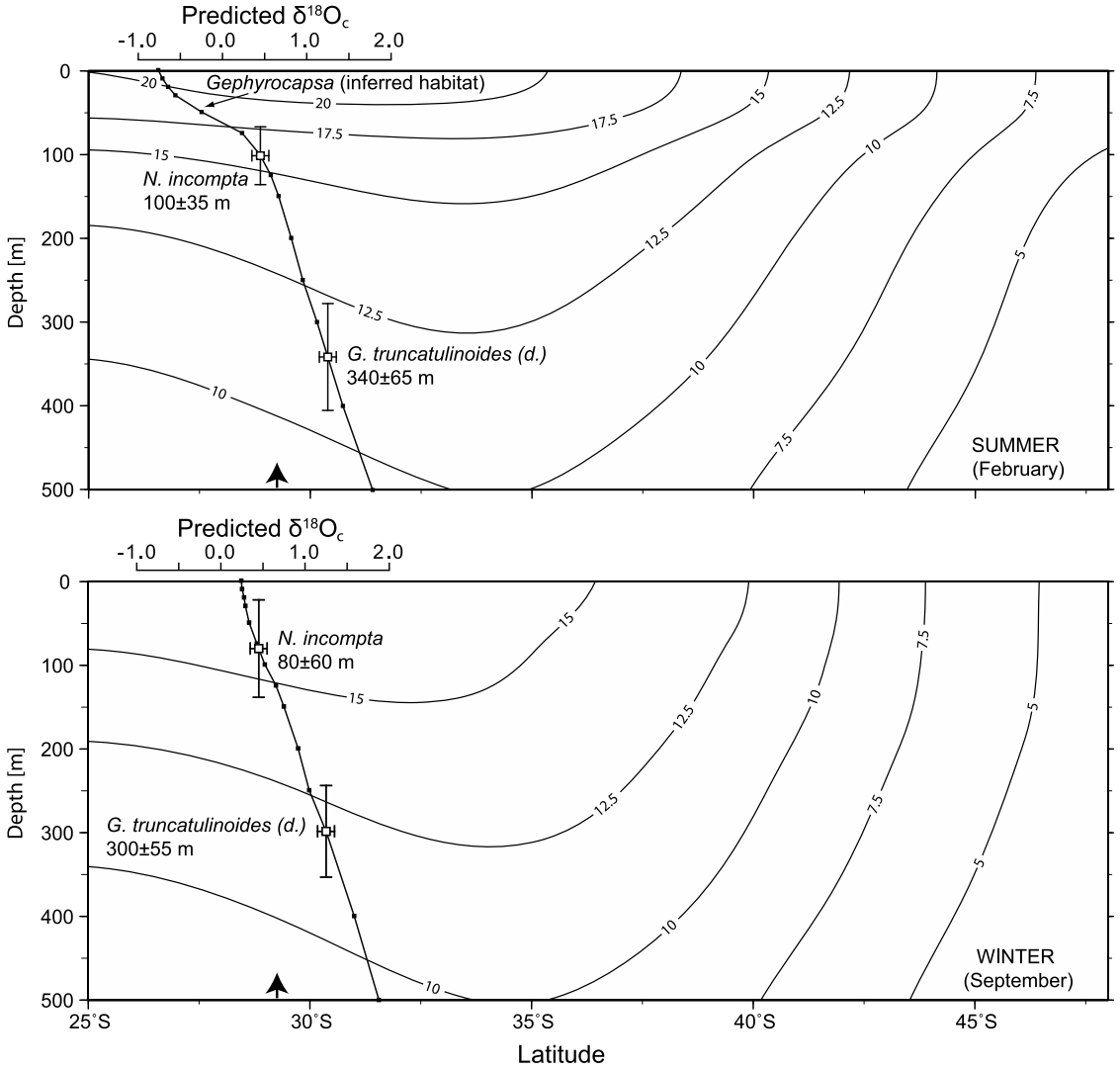

Figure 2. Predicted $\delta^{18}O_c$ profiles and estimated seasonal calcification depths for *N. incompta* and *G. truncatulinoides* (dextral) during austral summer and winter over Site 1085. Arrows denote the latitude of Site 1085. Isolines denote seawater temperatures [*Locarnini et al.*, 2006].

using a modern salinity-$\delta^{18}O_w$ relationship derived from a set of southeast Atlantic Ocean water samples (($\delta^{18}O_w = 0.416 \times SAL - 14.17$), $r^2 = 0.79$, $n = 15$ [*Schmidt et al.*, 1999]), which is close to the relationship found from whole ocean Geochemical Ocean Sections Study data. Values of $\delta^{18}O_w$ were converted to $\delta^{18}O_c$ using the *Locarnini et al.* [2006] water column temperatures and the *Kim and O'Neil* [1997] equilibrium calcite calibration (reexpressed by *Leng and Marshall* [2004]):

$$T(^\circ C) = 13.8 - 4.58(\delta_c - \delta_w) + 0.08(\delta_c - \delta_w)^2, \qquad (1)$$

where T is temperature. Values of $\delta^{18}O_c$ were converted from VSMOW to VPDB by subtracting 0.27‰ for consistency with previous studies [e.g., *Bemis et al.*, 1998]. Values of $\delta^{18}O_c$ were predicted for both summer (February) and winter (September) profiles (Figure 2).

[13] Core top values from GeoB1720-3 <500 years B.P. (on the basis of calibrated ^{14}C dates [*Dickson et al.*, 2009]) were averaged prior to matching them to the predicted $\delta^{18}O_c$ profiles to reduce the impact of samples affected by bioturbation on calcification depth estimates. No vital effect corrections were applied to the data, as both species calcify near to equilibrium at their depth abundance maxima in the southeastern Atlantic Ocean [*Mortyn and Charles*, 2003; *Lončarić et al.*, 2006]. Vertical (depth) error bars were estimated as the mean of the maximum and minimum depths that would be consistent with a change in foraminifera $\delta^{18}O_c$ values of ±0.2‰, estimated from a propagation of the $\delta^{18}O$ analytical error (<0.1‰) and the root-mean-square error from the southeast Atlantic Ocean surface water salinity-$\delta^{18}O_w$ relationship (0.17‰). Predicted $\delta^{18}O_c$ profiles do not vary substantially between summer and winter below the base of the summer thermocline (Figure 2), resulting in overlapping seasonal depth estimates of 100 ± 35 m (summer) and

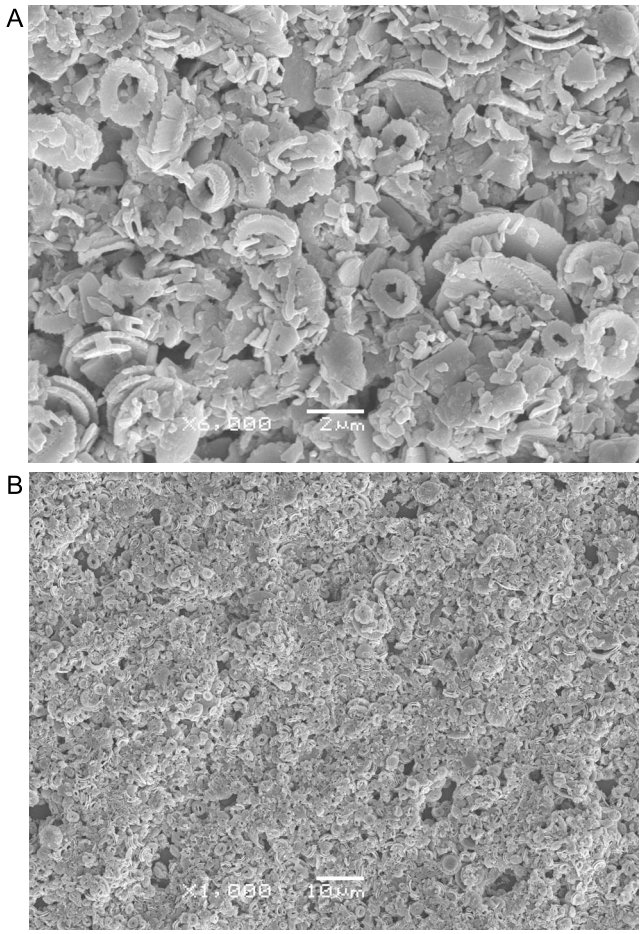

Figure 3. Scanning electron microscope images of the <63 μm fraction from sample 1085B-2H-5W-88 at (a) 6000X and (b) 1000X magnification. Material is dominated by small coccolithophore species of the genus *Gephyrocapsa*, with small contributions from *Coccolithus* spp. and *Calcidiscus* spp.

80 ± 60 m (winter) for *N. incompta* and 340 ± 65 m (summer) and 300 ± 55 m (winter) for *G. truncatulinoides* (dextral) (Figure 2). Inferred calcification depths for *G. truncatulinoides* (dextral) are in good agreement with those calculated using methods similar to those of *Lončarić et al.* [2006] on Walvis Ridge (200–350 m) and those modeled by *LeGrande et al.* [2004] using the assumption of a single calcification depth (~350 m). The calculated depth range for *N. incompta* is close to the base of the regional thermocline and, thus, is potentially controlled by the flux of organic matter from the surface of the euphotic zone [*Fairbanks et al.*, 1980; *Mortyn and Charles*, 2003].

[14] The slightly shallower inferred depth for *G. truncatulinoides* (dextral) during austral winter is consistent with observations that individuals of this species initially calcify at shallower depths before migrating to deeper levels as they mature [*Mulitza et al.*, 1997]. Lower δ^{18}O values of this species down core could therefore signify the effects of a shallower initial depth habitat consistent with a (seasonally) weaker thermocline and/or warming and/or freshening at subthermocline depths. The small differences in the inferred seasonal calcification depths in Figure 2 suggest that past changes in the temperature and salinity of subthermocline South Atlantic Central Waters (SACW), which currently fills the South Atlantic Ocean below the surface mixed layer to the boundary with underlying Antarctic Intermediate Water at ~700 m [*Siedler et al.*, 1996], should be the dominant influence.

3.2. Interpretation of Fine Carbonate δ^{18}O Values

[15] Stable oxygen isotope ratios measured on coccolith-dominated fine fraction carbonates have produced a number of stratigraphic curves that parallel recognized changes in seawater hydrography [e.g., *Margolis et al.*, 1975; *Anderson and Steinmetz*, 1981]. However, assemblage changes can potentially affect isotopic trends since different species of coccolithophore can secrete carbonate with δ^{18}O differences of up to 5‰ [*Dudley et al.*, 1986; *Ziveri et al.*, 2003]. Importantly, however, the magnitude of each species' vital effect seems to remain constant over a range of temperatures [*Ziveri et al.*, 2003]. Fine fraction isotope data can be further complicated by the presence of noncoccolith carbonate such as juvenile foraminifera, ostracods, or authigenic carbonates. Changes in coccolith species composition are not considered to compromise the reliability of the fine carbonate data from Site 1085. The middle Brunhes period between MIS 13 and 9 was dominated by blooms of the coccolithophore species *Gephyrocapsa caribbeanica*, which reached relative abundances of 70%–99% in deep-sea cores over large areas of the global ocean [*Bollmann et al.*, 1998]. This dominance has been reported from immediately north [*Baumann and Freitag*, 2004] and south [*Flores et al.*, 1999] of Site 1085, alongside other small *Gephyrocapsa* species such as *G. ericsonii* and *G. aperta* [*Baumann and Freitag*, 2004], which all follow a similar δ^{18}O offset from inorganic carbonate [*Dudley et al.*, 1986]. Large changes in species composition are not observed even over glacial-interglacial transitions, allowing an almost monospecific assemblage to dominate during the middle Brunhes. Scanning electron microscope investigations of several fine fraction (<63 μm) samples from Site 1085 qualitatively confirm the overwhelming dominance of small (<5 μm) *Gephyrocapsa* coccoliths through the study interval (Figure 3), alongside other coccolith species (e.g., *Coccolithus pelagicus* and *Calcidiscus leptoporus*) and larger carbonate material (e.g., foraminifera fragments) in small amounts. Therefore, although compositional changes undoubtedly introduce some analytical noise into the data, broad shifts in fine fraction isotope values should represent water column hydrography over Site 1085. Fine fraction δ^{18}O trends also match the pattern and amplitude of the planktonic foraminifera data, further suggesting that compositional assemblage changes have a minimal effect on δ^{18}O and δ^{13}C values [*Ennyu et al.*, 2002].

[16] Calcification depths of *Gephyrocapsa*-dominated fine fraction carbonate cannot be calibrated to modern hydrography using core top material because *Emiliania huxleyei* has dominated the coccolithophore assemblages of the southeastern Atlantic Ocean since ~260 ka [*Thierstein et al.*, 1977]. However, general information can be obtained from

published studies. Coccolithophores live in the upper photic zone where light, nutrients, and water column stability are optimal for growth [e.g., *Houghton*, 1988]. *G. oceanica* also dominates in surface sediments of the southeast Atlantic Ocean where the summer thermocline is strongly developed and temperatures are warm [*Giraudeau*, 1992]. However, this habitat preference is at odds with the raw $\delta^{18}O$ data, which are closer to values for *G. truncatulinoides* (dextral), implying calcification at depths up to 300 m or during times of upper ocean mixing in winter. This suggests that a species-dependent vital effect needs to be added to the fine fraction $\delta^{18}O$ values. Culture experiments have shown that small species of coccolithophores (including *G. oceanica*) produce calcite ~1.2‰ higher than equilibrium calcite [*Dudley et al.*, 1986; *Ziveri et al.*, 2003]. Consequently, this correction has been applied to the fine fraction $\delta^{18}O$ data in Figure 4. Since *E. huxleyei* and *G. oceanica* reproduce in large numbers at the end of periods of thermocline mixing when nutrient conditions are still elevated as the thermocline begins to stabilize [e.g., *Broerse et al.*, 2000], the fine carbonate $\delta^{18}O$ signal is interpreted as being biased toward near-surface waters during early spring. It is noted, however, that coccolith fluxes continue throughout the year in waters overlying Site 1085, making them broadly representative of upper ocean near-surface environments [*Romero et al.*, 2002].

3.3. $U^{K'}_{37}$ SST Estimates

[17] Core top $U^{K'}_{37}$ values from GeoB-1720-2 (17.6°C) and GeoB-1720-3 (16.1°C) are consistent with annual average Atlas temperatures at depths <50 m [*Locarnini et al.*, 2006] over the study site. This supports a statistical correlation between $U^{K'}_{37}$ and mean annual mixed layer temperatures (0–10 m) as suggested by *Müller and Fischer* [2003]. The redistribution of fine-grained material by bottom currents in the Benguela region has been demonstrated by *Mollenhauer et al.* [2003], but the similarity of down core $U^{K'}_{37}$ values with proxy data measured on different sedimentary fractions of coeval samples (Figure 4) suggests that this effect does not compromise the reliable interpretation of these data. Similar correspondence between alkenone and coarse fraction isotope data has also been found in other studies in the region [e.g., *Kirst et al.*, 1999; *Schneider et al.*, 1995]. It is likely that small age differences do exist owing to redistribution, but we do not consider these to unduly affect the interpretations that follow.

4. Results

[18] Each record shown in Figure 4 has a clear glacial-interglacial pattern, similar to the previously published benthic $\delta^{18}O$ record from the same sample suite [*Dickson et al.*, 2008]. The $\delta^{18}O$ values are higher during glacial periods MIS 12 and 10 and lower during MIS 11, with a glacial-interglacial range of ~1.7‰. Different suborbital $\delta^{18}O$ fluctuations characterize each $\delta^{18}O$ curve during and following MIS 11, suggesting a slightly different temperature and salinity response of surface and subsurface water masses through this period. Of particular note are several prominent ~0.75‰ decreases in *G. truncatulinoides* (dextral) $\delta^{18}O$ during the period 400–340 ka which are not seen in the *N. incompta* or fine fraction $\delta^{18}O$ records. The $U^{K'}_{37}$ record also follows a glacial-interglacial pattern with an amplitude of ~3°C. This is similar to the range of alkenone-inferred SST changes found over glacial terminations at other sites near Site 1085 [e.g., *Kirst et al.*, 1999; *Kim et al.*, 2002].

[19] Average $\delta^{18}O$ values in *N. incompta* and *G. truncatulinoides* (dextral) began to decrease subtly prior to the onset of termination 5, which is marked in the benthic $\delta^{18}O$ record as a sharp transition beginning at 431 ka and centered on 427 ka [*Lisiecki and Raymo*, 2005; *Dickson et al.*, 2008]. These subtle decreases took place between 440 and 424 ka for *N. incompta* and 443 and 425 ka for *G. truncatulinoides* (dextral), with magnitudes of ~0.5‰ and ~0.63‰, respectively. These subtle decreases were ended by more rapid decreases in $\delta^{18}O$ that marked the transition to full interglacial values (dashed line a in Figure 4). The early decreases in $\delta^{18}O$ parallel the early SST increase observed from 447 ka in the $U^{K'}_{37}$ data [*Dickson et al.*, 2009] but do not occur in the fine carbonate $\delta^{18}O$ data. This suggests that these $\delta^{18}O$ decreases/upper ocean warmings were either more pronounced in subsurface water masses and/or that the magnitude of the $\delta^{18}O$ change was reduced at near-surface depths by an increase in salinity that was relatively larger than at subthermocline depths. The distinct lag between the abrupt termination 5 $\delta^{18}O$ decrease observed in the benthic $\delta^{18}O$ record of Site 1085 [*Dickson et al.*, 2008] beginning at 431 ka [*Lisiecki and Raymo*, 2005] and the abrupt planktonic $\delta^{18}O$ decreases observed from ~425 ka suggest that the early part of the deglaciation (431–425 ka) was accompanied by elevated upper ocean salinity.

[20] The submillennial resolution of the Site 1085 data allows the identification of abrupt hydrographic events between MIS 12 and 10. The $U^{K'}_{37}$ SST records a series of millennial-scale warmings during the long-term cooling phase extending from the end of the warmest part of the MIS 11 optimum (404 ka according to the planktonic $\delta^{18}O$ data) to the MIS 10 glacial. These warmings were terminated by ~3.5°C cooling steps at 404, 390, 377, 362, and 346 ka (dashed lines b–e in Figure 4). Each SST peak is paralleled by a millennial-scale decrease in *G. truncatulinoides* (dextral) $\delta^{18}O$, with magnitudes between ~0.5‰ and 0.75‰. The LR04 benthic $\delta^{18}O$ curve does not exhibit similar variations during this period [*Lisiecki and Raymo*, 2005], suggesting that these events were driven by regional changes in SACW temperature and/or salinity. Assuming a temperature scaling of ~0.25‰/°C [*Leng and Marshall*, 2004], each $\delta^{18}O$ decrease is equivalent to ~2.5°C subthermocline warming. *N. incompta* $\delta^{18}O$ values do not record each of these events as consistently as *G. truncatulinoides* (dextral) values, although there is a clear similarity with $\delta^{18}O$ excursions centered at 380 and 353 ka. This may reflect the ability of *N. incompta* to migrate vertically in the water column in response to changes in the depth of the upper ocean productive zone [e.g., *Fairbanks et al.*, 1980; *Ortiz et al.*, 1995], thus reducing its sensitivity to water column temperature and salinity changes at a fixed depth. The large $\delta^{18}O$ decrease at 353 ka is found in all planktonic and benthic $\delta^{18}O$ records, suggesting a small decrease in global ice volume at this time. The greater

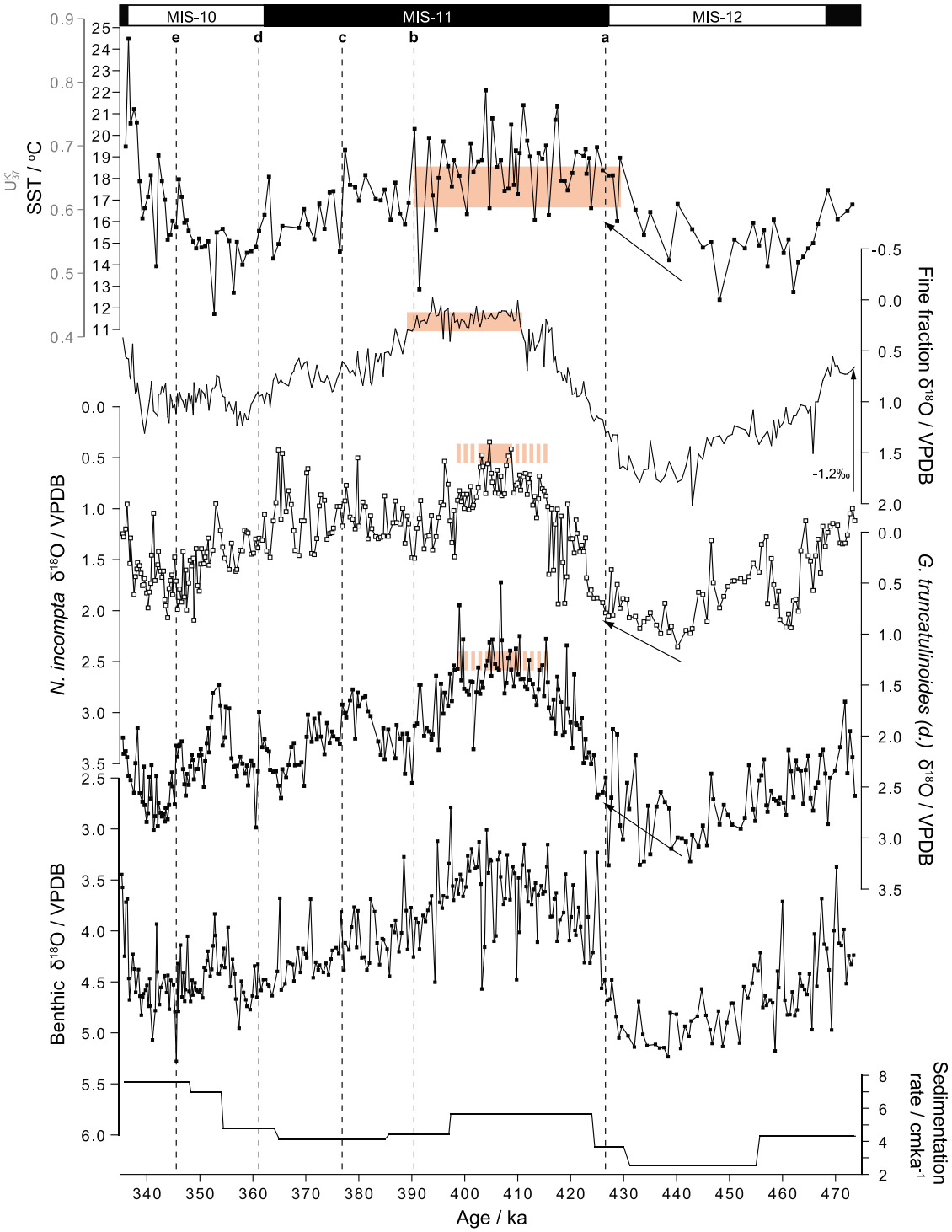

Figure 4. Stable isotope and $U^{K'}_{37}$ paleotemperature data from Site 1085 plotted on the LR04 age scale. Fine carbonate $\delta^{18}O$ values have been adjusted by −1.2‰ to account for a vital effect in small coccolithophore species [*Dudley et al.*, 1986]. Red-shaded bars reflect modern core top values (*y* axis, including an error of ±0.1‰) and the approximate duration over which "peak" values are maintained (*x* axis). No core top values exist for the fine fraction $\delta^{18}O$ data, and thus the red-shaded bar for this record denotes the average MIS 11 value. Arrows indicate the early upper ocean temperature increases observed prior to termination 5. Dashed lines a–e represent periods of inferred MOC strengthening during termination 5 and during millennial-scale events after the MIS 11 interglacial optimum.

magnitude of the $\delta^{18}O$ change for this event observed in the *G. truncatulinoides* (dextral) data implies additional amplification by subsurface warming or freshening over Site 1085.

[21] Abrupt changes in upper ocean hydrography are difficult to identify in the 40 ka period of MIS 12 prior to termination 5 because of the noise of the *G. truncatulinoides* (dextral) data and the reduced resolution of the alkenone data. Instead, this period is best exemplified by a gradual increase in *G. truncatulinoides* (dextral) $\delta^{18}O$ values between 475 and 440 ka. A large ~0.9‰ increase in $\delta^{18}O$ occurs in *N. incompta* between 464 and 458 ka but is not replicated in either of the other $\delta^{18}O$ records, suggesting that it may be an artifact of *N. incompta* ecology (e.g., seasonal and/or depth habitat changes). In summary, millennial-scale changes in seawater hydrography over Site 1085 appear to have been more pronounced during the MIS 11 and 10 glacial inception than during the MIS 13 and 12 inception.

5. Discussion

5.1. Duration of the MIS 11 Interglacial Optimum

[22] Previous studies have shown that peak warm conditions during the MIS 11 climatic optimum were maintained for an unusually long time. Estimates for the duration of this period converge on ~30,000 years, more than twice the duration of subsequent interglacial optimums [*Oppo et al.*, 1998; *Karner and Marra*, 2003; *McManus et al.*, 2003; *de Abreu et al.*, 2005; *Jouzel et al.*, 2007]. The different records shown in Figure 4, despite being plotted on the same age scale, appear to have recorded optimum climate conditions during MIS 11 for different durations. SSTs similar to or higher than the present day (17.6°C [*Locarnini et al.*, 2006]) were maintained for ~39,000 years between 429 and 390 ka. In contrast, $\delta^{18}O$ values fell within or below the range of modern core top values for a substantially shorter period of time. Low *G. truncatulinoides* (dextral) $\delta^{18}O$ values were maintained for ~18,000 years between 416 and 398 ka. However, this period was interrupted by brief ~0.2‰ excursions to higher values at 404 and 414 ka. When the intervening period alone is considered, stable low $\delta^{18}O$ values were only maintained for ~7000 years between 411 and 404 ka. *N. incompta* values were maintained at consistently low values of ~0.8‰ for ~17,000 years between 416 and 399 ka. However, as for *G. truncatulinoides* (dextral), values only fell within the late Holocene range for 6000 years between 409 and 403 ka. Fine sediment $\delta^{18}O$ remained constant at ~0.1‰–0.2‰ for 28,000 years between 417 and 389 ka, although the lack of core top data prevents a direct comparison of the magnitude of these values to the late Holocene. Taken together, these observations support the argument that the MIS 11 optimum was anomalously long but emphasize the point that the exact duration depends heavily on the type of proxy evidence used and the sampling resolution employed [*Hodell et al.*, 2000]. Comparing all four stratigraphies in Figure 4, the warmest interval of MIS 11 seems to have occurred for ~7000 years between 411 and 404 ka. It seems, however, that while SSTs may have been ~1°C on average warmer than during the Holocene [*Dickson et al.*, 2009], waters nearer the base of the thermocline recorded by *N. incompta* $\delta^{18}O$ may have been slightly cooler, assuming that the difference between modern and MIS 11 values is dominated by a temperature overprint. Alternatively, the ~0.2‰ higher MIS 11 values could represent higher seawater salinity of 0.5 practical salinity unit (PSU) (assuming a $\delta^{18}O$ against salinity gradient of ~0.5 [*Schmidt et al.*, 1999]). It is unlikely that seawater $\delta^{18}O$ was responsible for the slightly higher planktonic $\delta^{18}O$ values during MIS 11 since stacked benthic $\delta^{18}O$ data are on average 0.1‰ lower during the peak of MIS 11 (400–410 ka) than during the Holocene [*Lisiecki and Raymo*, 2005].

5.2. Mechanisms of Regional Hydrographic Changes: Influence of the MOC and Agulhas Leakage

[23] The southeast Atlantic Ocean is hydrographically complex, being affected by the upwelling of SACW close to the African coast, South Atlantic gyre waters at the boundaries of the upwelling zone, tropical Indian Ocean waters from the shedding of Agulhas rings, and subantarctic waters from large-scale eddy mixing at the subtropical front (STF) [*Garzoli and Gordon*, 1996; *Lutjeharms*, 1996]. The mixing of these different water masses can strongly influence the upper ocean temperature and salinity over the study site and is mainly controlled by the Agulhas Current strength and the position of the STF, which exerts a control on both Agulhas ring shedding and the northward advection of low-salinity subantarctic waters [*Gordon et al.*, 1992; *Garzoli and Gordon*, 1996; *Flores et al.*, 1999; *Peeters et al.*, 2004; *Cortese et al.*, 2007; *Biastoch et al.*, 2008; *Bard and Rickaby*, 2009]. Regional upper ocean temperature and salinity are also controlled by the rate of surface water advection northward within the Benguela Current. The leakage of Indian Ocean waters into the southeast Atlantic Ocean currently contributes ~25% of the 13–25 Sv transported northward by the Benguela Current [*Stramma and Peterson*, 1990; *Saunders and King*, 1995; *Garzoli and Gordon*, 1996], which acts as the principal conduit for moving surface waters away from the southeast Atlantic Ocean on the return limb of the MOC [*Zahn*, 2009]. A weakened MOC would therefore increase the upper ocean salinity of the study region given that the Agulhas leakage has continued unabated over the past 850,000 years [*Rau et al.*, 2006]. A weakened MOC would also contribute to regional upper ocean warming in response to a reduction in the ventilation of cold subsurface and intermediate waters coupled with the downward mixing of thermocline waters [*Wefer et al.*, 1996; *Rühlemann et al.*, 2004] and a reversal of cross-equatorial heat transport [*Chang et al.*, 2008]. Such warming seems to be most severe in subthermocline waters (SACW) [*Rühlemann et al.*, 2004].

[24] The following discussion is therefore based around a framework that simplifies the study region as a system whose near-surface salinity balance is dominantly governed by the balance between the rates of Agulhas leakage (input) and surface water export (output) within the Benguela Current and where the relationship of these regional effects to larger-scale MOC dynamics can be assessed through an examination of the subthermocline $\delta^{18}O$ (SACW warming) and benthic $\delta^{13}C$ data (North Atlantic Deep Water (NADW) advection to the study region) obtained from the same core stratigraphy. Variations in upper ocean temperature and salinity may also theoretically arise from changes in the atmospheric transport

of surface fresh water from the South Atlantic Ocean into the Pacific Ocean [*Gordon and Piola.*, 1983] and orbitally induced surface water warming in the tropics [e.g., *Sachs et al.*, 2001], but in the following discussion it is assumed that these influences were either constant or less important than the oceanographic processes that characterize the region.

[25] It has been suggested that the impact of the Agulhas leakage on the MOC is important during glacial terminations, when it may contribute to the sharp return of a strong "interglacial" mode of ocean circulation by adding to the Atlantic Ocean salt balance and thus overturning vigor [e.g., *Gordon*, 1996; *Weijer et al.*, 2002; *Knorr and Lohmann*, 2003; *Peeters et al.*, 2004]. Qualitative faunal indicators of the Agulhas leakage (ALF) from the Cape Basin (MD96-2081) [*Peeters et al.*, 2004] and from ODP Site 1087 [*Giraudeau et al.*, 2001] show a subtle increase prior to termination 5 during MIS 12 (Figure 5) but do not exhibit any dramatic increase in leakage that could have significantly increased the temperature and salinity budget of the regional upper ocean prior to termination 5 as suggested by decreasing *N. incompta* and *G. truncatulinoides* (dextral) $\delta^{18}O$ and increasing $U^{K'}_{37}$ SSTs and surface $\delta^{18}O_w$ at Site 1085. Consequently, the reduced northward advection of surface waters during MIS 12, coupled with the continuous (although reduced) input and accumulation of Agulhas waters [*Peeters et al.*, 2004; *Rau et al.*, 2006], likely drove the main part of the long-term SST and $\delta^{18}O_w$ increase over Site 1085 prior to termination 5.

[26] Upper ocean $\delta^{18}O_w$ and temperature over Site 1085 peaked suddenly at 430 ka following the MIS 12 maximum. It is likely that this sharp increase resulted from the southward movement of the STF which allowed an increased rate of Agulhas ring shedding into the southeast Atlantic Ocean, an argument supported by a corresponding increase in the abundance of *G. menardii* in Site 1087 [*Giraudeau et al.*, 2001] and in the abundance of ALF in MD96-2081 [*Peeters et al.*, 2004] (Figure 5). This $\delta^{18}O_w$ increase slightly preceded (by ~4000 years) an abrupt strengthening of the MOC recorded in the same core stratigraphy by an increase in normalized *G. truncatulinoides* (dextral) $\delta^{18}O$ values (and thus a fall in SACW temperatures) and a shift in benthic $\delta^{13}C$ to more positive values [*Dickson et al.*, 2008]. This sequence of events therefore suggests that (1) the rapid northward release of Agulhas leakage waters that had accumulated over the study region since 447 ka and (2) the increased rate of Agulhas ring shedding associated with the southward movement of the STF at 432 ka could have contributed to the rapid resumption of a warm interglacial mode of the MOC during MIS 11 at 427 ka, as suggested by *Gordon* [1996], *Peeters et al.* [2004], and *Cortese et al.* [2007]. This argument is supported by the observation that the high $\delta^{18}O_w$ values seen immediately following 430 ka do not plot along the modern South Atlantic Ocean and Indian Ocean $\delta^{18}O_w$ against temperature gradient shown in Figure 6 [*Schmidt et al.*, 1999] and thus cannot be explained by the mixing of modern water masses in these ocean basins. Such values require a source of warm, highly saline waters to have influenced the region during and following termination 5, such as those hypothesized to have been generated within the highly evaporative Indian Ocean during glacial periods and subsequently released as the Agulhas leakage intensified during deglaciations [e.g., *Peeters*, 2008].

[27] The millennial-scale warming events observed during the MIS 11 and 10 transition over Site 1085 (Figure 4) are consistent with previous observations of South Atlantic Ocean hydrological changes in response to a reduction in MOC intensity. This consistency arises from (1) the similarity between the magnitude of SST and inferred SACW warming (~2°C–3°C) with warming events observed during abrupt Northern Hemisphere cooling and Southern Hemisphere warming events during the last glacial cycle [e.g., *Rühlemann et al.*, 1999], as well as the magnitude of regional upper ocean warming predicted by numerical models, which fall in the same range [*Rühlemann et al.*, 2004; *Chang et al.*, 2008], (2) the correspondence of each SST increase with an increase in sea surface $\delta^{18}O_w$ (salinity), which is also consistent with the predicted impact of a decrease in MOC intensity on regional surface ocean hydrography, (3) the sharp SST and $\delta^{18}O_w$ decreases observed over Site 1085 during the MIS 11 and 10 glacial inception, which are not consistent with a linear response to insolation forcing but could be explained by an abrupt increase in the advection of warm, saline surface waters away from the region in the return limb of the MOC [*Weijer et al.*, 2002; *Knorr and Lohmann*, 2003], and (4) the correspondence between each upper ocean SST and $\delta^{18}O_w$ increase with low benthic $\delta^{13}C$ values in Site 1085, which could reflect a reduction in the mass or rate of NADW advection to the middepth southeast Atlantic Ocean [*Dickson et al.*, 2008], thus suggesting a precise phasing between abrupt increases in southeast Atlantic Ocean temperature and salinity and decreased MOC intensity. It is therefore likely that the stepped decreases in southeast Atlantic temperature and salinity that took place during the MIS 11 and 10 glacial inception were forced mechanistically by strengthening of the return limb of the MOC. A further point to note is that the end of each warming event coincided with a sharp increase in benthic $\delta^{13}C$ values, suggesting an increase in the mass or rate of NADW transport to the middepth South Atlantic (Figure 5).

[28] Although MOC variability may explain the occurrence of these brief events, it does not fully explain the magnitude of the $\delta^{18}O_w$ responses. Numerical modeling predicts a sea surface salinity increase of ~0.1–0.2 PSU over Site 1085 resulting from a sudden decrease in MOC overturning [*Rühlemann et al.*, 2004], but assuming a $\delta^{18}O_w$ against salinity scaling of 0.5‰/PSU, this mechanism would only account for ~0.05‰–0.1‰ of the ~0.5‰ $\delta^{18}O_w$ change observed during each event. The most likely explanation for these observations is the strong presence of saline Indian Ocean waters over the core location during the surface warming events of the MIS 11 and 10 transition. Data for these events plot close to the modern $\delta^{18}O_w$ against temperature mixing line in Figure 6 and so would simply require increased mixing of Indian Ocean waters rather than the sudden release of highly saline "glacial" Indian Ocean waters as inferred for the early part of MIS 11 following termination 5. Such an interpretation is also supported by the correspondence between SST and $\delta^{18}O_w$ peaks at Site 1085 with peaks in the abundance of *G. menardii* at Site 1087 [*Giraudeau et al.*, 2001] (Figure 5), suggesting a slightly

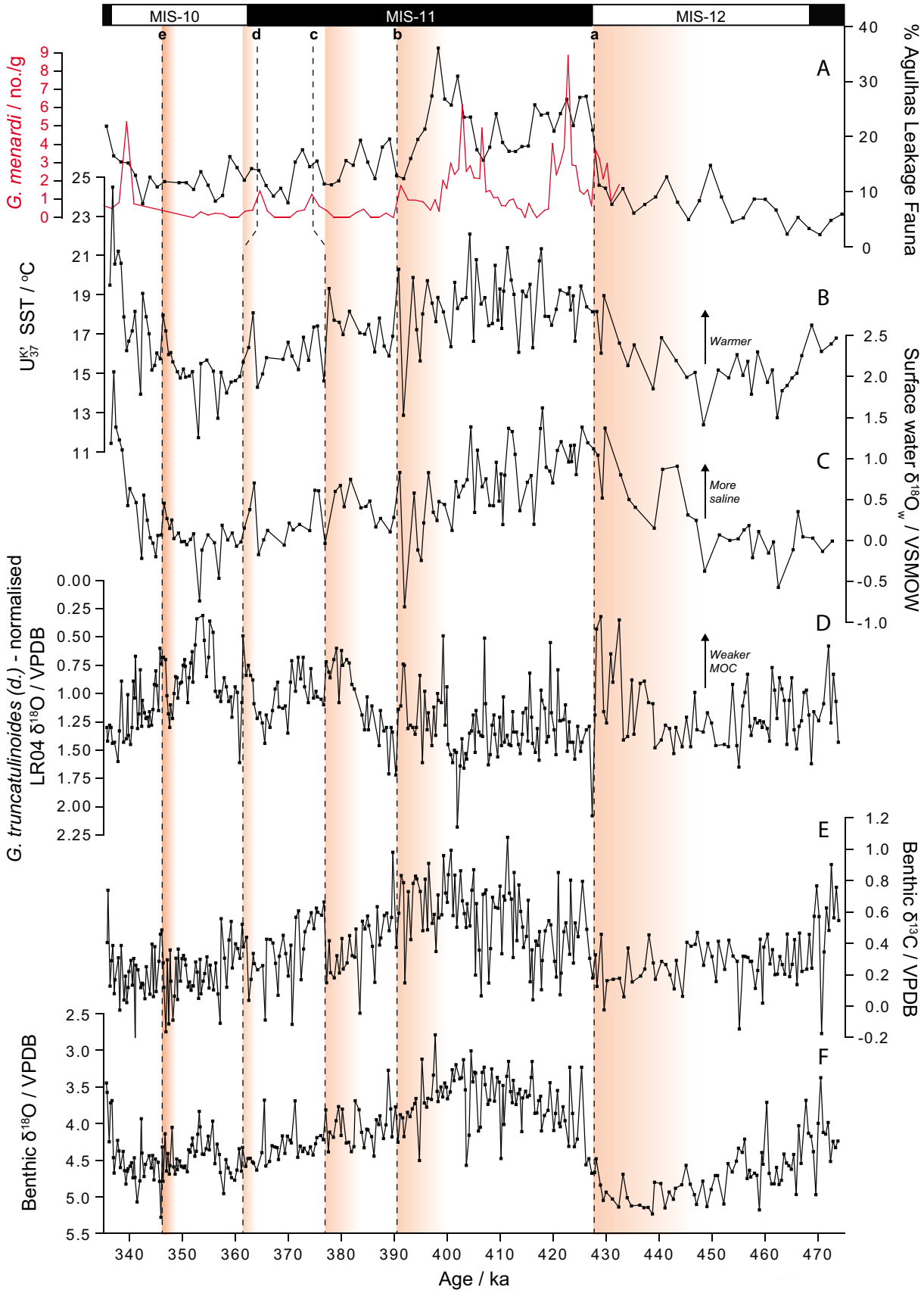
MIS-10
MIS-11
MIS-12
e
d
c
b
a
A
B
C
D
E
F
G. menardi / no./g
% Agulhas Leakage Fauna
U^K'37 SST / °C
Warmer
More saline
Surface water δ18Ow / VSMOW
G. truncatulinoides (d.) - normalised LR04 δ18O / VPDB
Weaker MOC
Benthic δ13C / VPDB
Benthic δ18O / VPDB
Age / ka

Figure 5

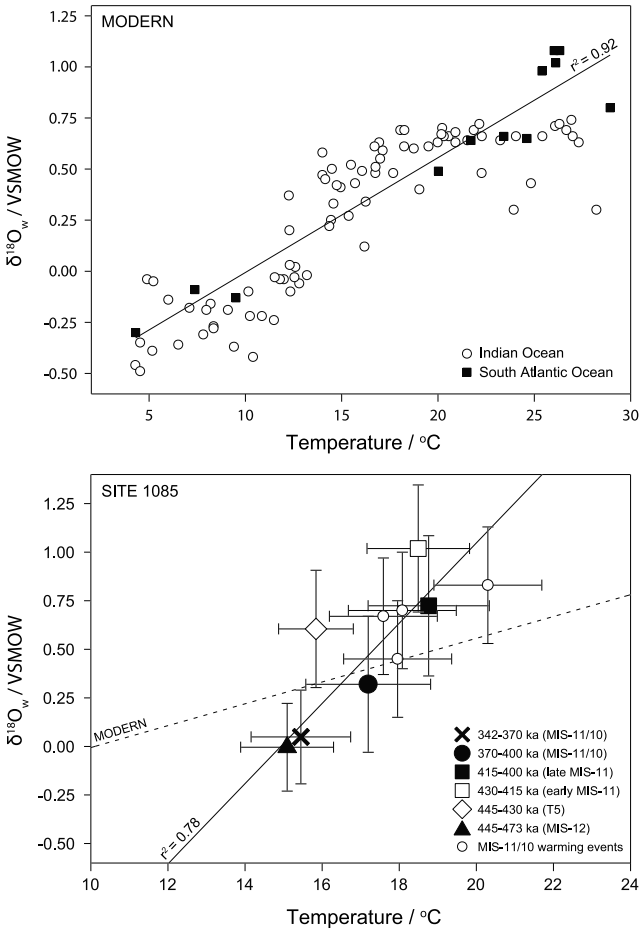

Figure 6. Temperature-$\delta^{18}O^{w}$ relationships for (top) modern South Atlantic and Indian Ocean surface (0–10 m) waters [*Schmidt et al.*, 1999] and (bottom) ODP Site 1085 proxy data (this study). Linear relationship shown in Figure 6 (top) is for South Atlantic waters only, and the linear relationship in Figure 6 (bottom) is for all Site 1085 data.

enhanced rate of Agulhas leakage during these millennial-scale events. Assuming these correlations are "real," i.e., within the precision of temporal correlation between sites 1085 and 1087, one explanation for their occurrence could be a slight southward shift in the latitude of the STF during Northern Hemisphere millennial-scale cooling and Southern Hemisphere warming intervals that allowed an increased rate of Agulhas ring shedding [e.g., *Barker et al.* 2009], a mechanism consistent with the inferred pattern of atmospheric circulation over southern Africa during this interval (Dickson et al., Oceanic, atmospheric and ice-sheet forcing of southeast Atlantic Ocean productivity and south African monsoon intensity during MIS-12 to 10, 2009). The increases in upper ocean temperature and $\delta^{18}O_w$ over Site 1085 during the MIS 11 and 10 transition are therefore attributed to weakened surface water export coupled with the progressive addition of Agulhas waters. It is possible that the gradual accumulation of Agulhas-derived salinity during each of these periods could have contributed to subsequent abrupt intensifications of the Benguela Current, as it was advected throughout the tropical Atlantic Ocean [*Weijer et al.*, 2002; *Biastoch et al.*, 2008], ultimately acting as a negative salinity feedback on millennial-scale MOC slowdowns.

[29] A curious feature of MIS 11 that is not found in later interglacials is a second peak in Agulhas leakage fauna toward the end of the interglacial optimum in Cape Basin faunal records [*Giraudeau et al.*, 2001; *Peeters et al.*, 2004]. This feature has some significant differences from the faunal peaks during termination 5 and during the MIS 11and 10 transition, in that there is no associated increase in near-surface temperature and salinity over Site 1085 (Figure 5). The Southern Hemisphere frontal systems may have started to migrate northward in response to cooling in the Southern Ocean after 415 ka [*Kunz-Pirrung et al.*, 2002], which makes it difficult to envisage a southward shift in the STF [*Cortese et al.*, 2007] as the primary mechanism for this second peak in Agulhas leakage. One possibility is that interocean exchange was enhanced at the end of the MIS 11 optimum by a strengthening of the regional trade winds. This mechanism would be consistent with an increase in south African monsoon intensity, reflecting stronger Indian Ocean trade winds (Dickson et al., submitted manuscript, 2009) and a rapid export of near-surface waters out of the southeast Atlantic Ocean by a strengthened Benguela Current. The latter suggestion is supported by lower $\delta^{18}O_w$ values and higher normalized *G. truncatulinoides* (dextral) $\delta^{18}O$ values over Site 1085 (recording lower near-surface salinity and cooler SACW) and a reduction in the proportion of "warmer" deep-dwelling *G. truncatulinoides* (dextral) in ODP Site 1087 compared to the termination 5 Agulhas leakage event (also reflecting cooler subthermocline waters [*Giraudeau et al.*, 2001]). Although consistent with the simple salinity input-output model outlined above, it is suggested here that a strengthened Agulhas leakage was able to positively feed back on a strong MOC at that time, whereas in the other intervals (termination 5, MIS 11and 10 transition) it acted more as a negative feedback on a weakened MOC. This enhanced "warm water" return flow could ultimately have

Figure 5. Upper ocean hydrographic variability over Site 1085 between 475 and 335 ka plotted on the LR04 age scale. (a) Concentrations of the planktonic foraminifera *Globoratalia menardii* in ODP Site 1087 (red line) [*Giraudeau et al.*, 2001] and percent of Agulhas Leakage fauna in MD96-2081 (black line) [*Peeters et al.*, 2004]. (b) Site 1085 SST. (c) Site 1085 surface water $\delta^{18}O_w$ derived from SST and fine-carbonate $\delta^{18}O$. (d) Site 1085 *G. truncatulinoides* (d.) $\delta^{18}O$ residuals following subtraction of normalized whole ocean values from the LR04 stack (see the auxiliary material). (e and f) Site 1085 benthic $\delta^{13}C$ and $\delta^{18}O$, respectively [*Dickson et al.*, 2008]. Sites 1087 and MD96-2081 have been placed on the LR04 age scale by retuning their respective benthic $\delta^{18}O$ records (see methods in Text S1) [*Pierre et al.*, 2001; *Peeters et al.*, 2004]. Dashed vertical lines a–e are the same as in Figure 4.

supplied the moisture necessary for Northern Hemisphere ice sheet growth following the MIS 11 and 10 glacial inception at ~397 ka [*Müller and Pross*, 2007].

6. Conclusion

[30] Stable oxygen isotope and alkenone data from ODP Site 1085 provide new, submillennial-scale resolution records of southeast Atlantic upper ocean hydrographic changes during the period ~475–335 ka. Although warm interglacial SSTs (~18.5°C) were maintained for ~39,000 years during MIS 11, minimum $\delta^{18}O$ values in planktonic foraminifera suggest a much shorter peak interglacial lasting for ~7000 years between ~411 and 404 ka according to the applied age model. *N. incompta* $\delta^{18}O$ values during the MIS 11 interglacial were generally higher than during the Holocene, suggesting either slightly cooler subsurface waters or an ecological shift in species habitat between the two periods. Surface salinity and temperature variations over Site 1085 are considered to mainly reflect the balance between the input of water masses (Agulhas waters, subantarctic surface waters) and their subsequent rate of export within the northward flowing return limb of the MOC (Benguela Current). Although regional increases in upper ocean temperature and salinity prior to termination 5 and during millennial-scale events following MIS 11 are consistent with a weakened MOC, and thus in the rate of surface water export, they were likely amplified by additions of warm, salty Agulhas leakage waters. These additions may have eventually acted as a negative salinity feedback on the initial MOC slowdown, triggering rapid resumptions of the MOC as surface waters were released northward from the tropical Atlantic Ocean [e.g., *Knorr and Lohmann*, 2003; *Schmidt et al.*, 2006]. A second peak of Agulhas leakage suggested to have occurred during the end of the MIS 11 interglacial optimum [*Peeters et al.*, 2004] is not clearly expressed in Site 1085 surface salinity data, probably because of a vigorous northward export of near-surface waters at that time. A strong Agulhas leakage could therefore have helped to maintain a strong MOC during the initial part of the MIS 11 to 10 glacial inception, thus contributing to Northern Hemisphere ice sheet buildup.

[31] **Acknowledgments.** We wish to thank Ian Harrison and Janet Hope for laboratory support and Paul Bown for advice on coccolith taxonomy. This work was supported by a NERC CASE Ph.D. studentship (NER/S/A/2005/13226) awarded to A.J.D., NIGSF award IP/894/0506, and NERC Life Science Mass Spectrometry Facility award lsmsfbris008. All data will be archived within the NOAA National Climatic Data center (available at http://www.ncdc.noaa.gov/paleo/paleo.html).

References

Anderson, T. F., and J. C. Steinmetz (1981), Isotopic and biostratigraphical records of calcareous nannofossils in a Pleistocene core, *Nature*, *294*, 741–744, doi:10.1038/294741a0.

Bard, E., and R. E. M. Rickaby (2009), Migration of the subtropical front as a modulator of glacial climate, *Nature*, *460*, 380–383, doi:10.1038/nature08189.

Barker, S., P. Diz, M. J. Vautravers, J. Pike, G. Knorr, I. R. Hall, and W. S. Broecker (2009), Interhemispheric Atlantic seesaw response during the last deglaciation, *Nature*, *457*, 1097–1102, doi:10.1038/nature07770.

Baumann, K. H., and T. Freitag (2004), Pleistocene fluctuations in the northern Benguela Current system as revealed by coccolith assemblages, *Mar. Micropaleontol.*, *52*, 195–215, doi:10.1016/j.marmicro.2004.04.011.

Beltran, C., M. de Rafelis, F. Minoletti, M. Renard, M. A. Sicre, and U. Ezat (2007), Coccolith $\delta^{18}O$ and alkenone records in middle Pliocene orbitally controlled deposits: High-frequency temperature and salinity variations of sea surface water, *Geochem. Geophys. Geosyst.*, *8*, Q05003, doi:10.1029/2006GC001483.

Bemis, B. E., H. J. Spero, J. Bijima, and D. W. Lea (1998), Reevaluation of the oxygen isotope composition of planktonic foraminifera: Experimental results and revised paleotemperature equations, *Paleoceanography*, *13*, 150–160, doi:10.1029/98PA00070.

Berger, A., and M. F. Loutre (2002), An exceptionally long interglacial ahead?, *Science*, *297*, 1287–1288, doi:10.1126/science.1076120.

Biastoch, A., C. W. Boning, and J. R. E. Lutjeharms (2008), Agulhas leakage dynamics affects decadal variability in Atlantic overturning circulation, *Nature*, *456*, 489–492, doi:10.1038/nature07426.

Billups, K., W. Chaisson, M. Worsnopp, and R. Thunell (2004), Millennial-scale fluctuations in subtropical northwestern Atlantic surface ocean hydrography during the mid-Pleistocene, *Paleoceanography*, *19*, PA2017, doi:10.1029/2003PA000990.

Bollmann, J., K. H. Baumann, and H. R. Thierstein (1998), Global dominance of *Gephyrocapsa* coccoliths in the late Pleistocene: Selective dissolution, evolution, or global environmental change?, *Paleoceanography*, *13*, 517–529, doi:10.1029/98PA00610.

Broerse, A. T. C., G.-J. A. Brummer, and J. E. Van Hinte (2000), Coccolithophore export production in response to monsoonal upwelling off Somalia (northwestern Indian Ocean), *Deep Sea Res., Part II*, *47*, 2179–2205, doi:10.1016/S0967-0645(00)00021-7.

Chang, P., R. Zhang, W. Hazerleger, C. Wen, X. Wan, L. Ji, R. J. Haarsma, W. P. Breugem, and H. Seidel (2008), Oceanic link between abrupt changes in the North Atlantic Ocean and the African monsoon, *Nat. Geosci.*, *1*, 444–448, doi:10.1038/ngeo218.

Cléroux, C., E. Cortijo, J.-C. Duplessy, and R. Zahn (2007), Deep-dwelling foraminifera as thermocline temperature recorders, *Geochem. Geophys. Geosyst.*, *8*, Q04N11, doi:10.1029/2006GC001474.

Conte, M. H., M.-A. Sicre, C. Ruhlemann, J. C. Weber, S. Schulte, D. Schultz-Bull, and T. Blanz (2006), Global temperature calibration of the alkenone unsaturation index ($U^{K'}_{37}$) in surface waters and comparison with surface sediments, *Geochem. Geophys. Geosyst.*, *7*, Q02005, doi:10.1029/2005GC001054.

Cortese, G., A. Abelmann, and R. Gersonde (2007), The last five glacial-interglacial transitions: A high-resolution 450,000-year record from the subantarctic Atlantic, *Paleoceanography*, *22*, PA4203, doi:10.1029/2007PA001457.

Darling, K. F., M. Kucera, D. Kroon, and C. M. Wade (2006), A resolution for the coiling direction paradox in *Neogloboquadrina pachyderma*, *Paleoceanography*, *21*, PA2011, doi:10.1029/2005PA001189.

de Abreu, L., F. F. Abrantes, N. J. Shackleton, P. C. Tzedakis, J. F. McManus, D. W. Oppo, and M. A. Hall (2005), Ocean climate variability in the eastern North Atlantic during marine isotope stage 11: A partial analogue to the Holocene?, *Paleoceanography*, *20*, PA3009, doi:10.1029/2004PA001091.

de Vargas, C., S. Renaud, H. Hillbrecht, and J. Pawlowski (2001), Pleistocene adaptive radiation in *Globoratalia truncatulinoides*: Genetic, morphologic, and environmental evidence, *Paleobiology*, *27*, 104–125, doi:10.1666/0094-8373(2001)027<0104:PARIGT>2.0.CO;2.

Dickson, A. J., M. J. Leng, and M. A. Maslin (2008), Mid-depth South Atlantic Ocean circulation and chemical stratification during MIS-10 to 12: Implications for atmospheric CO_2, *Clim. Past*, *4*, 333–344, doi:10.5194/cp-4-333-2008.

Dickson, A. J., C. J. Beer, C. Dempsey, J. A. Bendle, M. A. Maslin, E. L. McClymont, and R. D. Pancost (2009), Oceanic forcing of the marine isotope stage 11 interglacial, *Nat. Geosci.*, *2*, 428–433, doi:10.1038/ngeo527.

Dudley, W. C., P. Blackwelder, L. Brand, and J. C. Duplessy (1986), Stable isotopic composition of coccoliths, *Mar. Micropaleontol.*, *10*, 1–8, doi:10.1016/0377-8398(86)90021-6.

Ennyu, A., M. A. Arthur, and M. Pagani (2002), Fine-fraction carbonate stable isotopes as indicators of seasonal shallow mixed-layer paleohydrography, *Mar. Micropaleontol.*, *46*, 317–342, doi:10.1016/S0377-8398(02)00079-8.

EPICA Community Members (2004), Eight glacial cycles from an Antarctic ice core, *Nature*, *429*, 623–628, doi:10.1038/nature02599.

Fairbanks, R. G., P. H. Wiebe, and A. W. H. Be (1980), Vertical distribution and isotopic

composition of living planktonic foraminifera in the western North Atlantic, *Science*, *207*, 61–63, doi:10.1126/science.207.4426.61.

Flores, J.-A., R. Gersonde, and F. J. Sierro (1999), Pleistocene fluctuations in the Agulhas Current retroflection based on the calcareous plankton record, *Mar. Micropaleontol.*, *37*, 1–22, doi:10.1016/S0377-8398(99)00012-2.

Garzoli, S. L., and A. L. Gordon (1996), Origins and variability of the Benguela Current, *J. Geophys. Res.*, *101*(C1), 897–906, doi:10.1029/95JC03221.

Giraudeau, J. (1992), Distribution of recent nannofossils beneath the Benguela system: Southwest African continental margin, *Mar. Geol.*, *108*, 219–237, doi:10.1016/0025-3227(92)90174-G.

Giraudeau, J., C. Pierre, and L. Herve (2001), A late-Quaternary, high resolution record of planktonic foraminiferal species distribution in the southern Benguela region: Site 1087, *Proc. Ocean Drill. Program Sci. Results*, *175*, 1–26.

Gordon, A. J. (1996), Comment on the South Atlantic's role in the global circulation, in *The South Atlantic: Present and Past Circulation*, edited by G. Wefer et al., pp. 121–124, Springer, Berlin.

Gordon, A. L., and A. R. Piola (1983), Atlantic Ocean upper layer salinity budget, *J. Phys. Oceanogr.*, *13*, 1293–1300, doi:10.1175/1520-0485(1983)013<1293:AOULSB>2.0.CO;2.

Gordon, A. L., R. F. Weiss, W. M. Smethie Jr., and M. J. Warner (1992), Thermocline and intermediate water communication between the South Atlantic and Indian oceans, *J. Geophys. Res.*, *97*(C5), 7223–7240, doi:10.1029/92JC00485.

Hodell, D. A., C. D. Charles, and U. S. Ninnemann (2000), Comparison of interglacial stages in the south Atlantic sector of the Southern Ocean for the past 450 kyr: Implications for marine isotope stage (MIS) 11, *Global Planet. Change*, *24*, 7–26, doi:10.1016/S0921-8181(99)00069-7.

Hodell, D. A., S. Kanfoush, K. A. Venz, and C. D. Charles (2003), The mid-Brunhes transition in ODP sites 1989 and 1090 (subantarctic South Atlantic), in *Earth's Climate and Orbital Eccentricity: The Marine Isotope Stage 11 Question*, *Geophys. Monogr. Ser.*, vol. 137, edited by A. W. Droxler, R. Z. Poore, and L. H. Burckle, pp. 113–129, AGU, Washington, D. C.

Houghton, S. D. (1988), Thermocline control on coccolith diversity and abundance in recent sediments from the Celtic Sea and English Channel, *Mar. Geol.*, *83*, 313–319, doi:10.1016/0025-3227(88)90065-5.

Jouzel, J., et al. (2007), Orbital and millennial Antarctic climate variability over the past 800,000 years, *Science*, *317*, 793–796, doi:10.1126/science.1141038.

Kandiano, E. S., and H. A. Bauch (2007), Phase relationship and surface water mass change in the northeast Atlantic during marine isotope stage 11 (MIS 11), *Quat. Res.*, *68*, 445–455, doi:10.1016/j.yqres.2007.07.009.

Karner, D. B., and F. Marra (2003), $^{40}Ar/^{39}Ar$ dating of glacial termination V and the duration of marine isotopic stage 11, in *Earth's Climate and Orbital Eccentricity: The Marine Isotope Stage 11 Question*, *Geophys. Monogr. Ser.*, vol. 137, edited by A. W. Droxler, R. Z. Poore, and L. H. Burckle, pp. 61–66, AGU, Washington, D. C.

Kim, J.-H., R. R. Schneider, P. J. Müller, and G. Wefer (2002), Interhemispheric comparison of deglacial sea-surface temperature patterns in Atlantic eastern boundary currents, *Earth Planet. Sci. Lett.*, *194*, 383–393, doi:10.1016/S0012-821X(01)00545-3.

Kim, S.-T., and J. R. O'Neil (1997), Equilibrium and nonequilibrium oxygen isotope effects in synthetic carbonates, *Geochim. Cosmochim. Acta*, *61*, 3461–3475, doi:10.1016/S0016-7037(97)00169-5.

Kirst, G. J., R. R. Schneider, P. J. Muller, I. von Storch, and G. Wefer (1999), Late Quaternary temperature variability in the Benguela Current system derived from alkenones, *Quat. Res.*, *52*, 92–103, doi:10.1006/qres.1999.2040.

Knorr, G., and G. Lohmann (2003), Southern Ocean origin for the resumption of Atlantic thermohaline circulation during deglaciation, *Nature*, *424*, 532–536, doi:10.1038/nature01855.

Kunz-Pirrung, M., R. Gersonde, and D. A. Hodell (2002), Mid-Brunhes century-scale diatom sea surface temperature and sea ice records from the Atlantic sector of the Southern Ocean (ODP Leg 177, sites 1093, 1094 and core PS2089-2), *Palaeogeogr. Palaeoclimatol. Palaeoecol.*, *182*, 305–328, doi:10.1016/S0031-0182(01)00501-6.

LeGrande, A. N., J. Lynch-Stieglitz, and E. C. Farmer (2004), Oxygen isotopic composition of *Globoratalia truncatulinoides* as a proxy for intermediate depth density, *Paleoceanography*, *19*, PA4025, doi:10.1029/2004PA001045.

Leng, M. J., and J. D. Marshall (2004), Paleoclimate interpretation of stable isotope data from lake sediment archives, *Quat. Sci. Rev.*, *23*, 811–831, doi:10.1016/j.quascirev.2003.06.012.

Lisiecki, L. E., and M. E. Raymo (2005), A Pliocene-Pleistocene stack of 57 globally distributed benthic $\delta^{18}O$ records, *Paleoceanography*, *20*, PA1003, doi:10.1029/2004PA001071.

Locarnini, R. A., A.V. Mishonov, J. I. Antonov, T. P. Boyer, H. E. Garcia, and S. Levitus (2006), *World Ocean Atlas 2005*, vol. 1, *Temperature*, *NOAA Atlas NESDIS*, vol. 61, edited by S. Levitus, 182 pp., NOAA, Silver Spring, Md.

Lončarić, N., F. J. C. Peeters, D. Kroon, and G.-J. A. Brummer (2006), Oxygen isotope ecology of recent planktic foraminifera at the central Walvis Ridge (SE Atlantic), *Paleoceanography*, *21*, PA3009, doi:10.1029/2005PA001207.

Loutre, M.-F., and A. Berger (2003), Marine isotope stage 11 as an analogue for the present interglacial, *Global Planet. Change*, *36*, 209–217, doi:10.1016/S0921-8181(02)00186-8.

Lutjeharms, J. R. E. (1996), The exchange of water between the South Indian and the South Atlantic, in *The South Atlantic: Present and Past Circulation*, edited by G. Wefer et al., pp. 125–162, Springer, Berlin.

Lutjeharms, J. R. E. (2006), *The Agulhas Current*, 329 pp., Springer, Berlin.

Lutjeharms, J. R. E., F. A. Shillington, and C. M. Duncombe-Rae (1991), Observations of extreme upwelling filaments in the southeast Atlantic Ocean, *Science*, *253*, 774–776, doi:10.1126/science.253.5021.774.

Margolis, S. V., P. M. Kroopnick, D. E. Goodney, W. C. Dudley, and M. E. Mahoney (1975), Oxygen and carbon isotopes from calcareous nannofossils as paleoceanographic indicators, *Science*, *189*, 555–557, doi:10.1126/science.189.4202.555.

Martrat, B., J. O. Grimalt, N. J. Shackleton, L. de Abreu, M. A. Hutterli, and T. F. Stocker (2007), Four climate cycles of recurring deep and surface water destabilizations on the Iberian margin, *Science*, *317*, 502–507, doi:10.1126/science.1139994.

McKenna, V. S., and W. L. Prell (2004), Calibration of the Mg/Ca of *Globorotalia truncatulinoides* (R) for the reconstruction of marine temperature gradients, *Paleoceanography*, *19*, PA2006, doi:10.1029/2000PA000604.

McManus, J. F., D. W. Oppo, J. Cullen, and S. Healey (2003), Marine isotope stage 11 (MIS-11): Analog for Holocene and future climate?, in *Earth's Climate and Orbital Eccentricity: The Marine Isotope Stage 11 Question*, *Geophys. Monogr. Ser.*, vol. 137, edited by A. Droxler, R. Z. Poore, and L. H. Burckle, pp. 69–85, AGU, Washington, D. C.

Mollenhauer, G., T. I. Eglinton, N. Ohkouchi, R. R. Schneider, P. J. Muller, P. M. Grootes, and J. Rullkotter (2003), Asynchronous alkenone and foraminifera records from the Benguela upwelling system, *Geochim. Cosmochim. Acta*, *67*, 2157–2171, doi:10.1016/S0016-7037(03)00168-6.

Mortyn, P. G., and C. D. Charles (2003), Planktonic foraminiferal depth habitat and $\delta^{18}O$ calibrations: Plankton tow results from the Atlantic sector of the Southern Ocean, *Paleoceanography*, *18*(2), 1037, doi:10.1029/2001PA000637.

Mulitza, S., A. Duerkoop, W. Hale, G. Wefer, and H. S. Niebler (1997), Planktonic foraminifera as recorders of past surface-water stratification, *Geology*, *25*, 335–338, doi:10.1130/0091-7613(1997)025<0335:PFAROP>2.3.CO;2.

Mulitza, S., D. Boltovskoy, B. Donner, H. Meggers, A. Paul, and G. Wefer (2003), Temperature: $\delta^{18}O$ relationships of planktic foraminifera collected from surface waters, *Palaeogeogr. Palaeoclimatol. Palaeoecol.*, *202*, 143–152, doi:10.1016/S0031-0182(03)00633-3.

Müller, P. J., and G. Fischer (2003), C_{37}-Alkenones as paleotemperature tool: Fundamentals based on sediment traps and surface sediments from the South Atlantic Ocean, in *The South Atlantic in the Late Quaternary: Reconstruction of Material Budgets and Current Systems*, edited by G. Wefer, S. Mulitza, and V. Ratmeyer, pp. 167–193, Springer, Berlin.

Müller, P. J., G. Kirst, G. Ruhland, I. von Storch, and A. Rosell-Mele (1998), Calibration of the alkenone palaeotemperature index $U^{K'}_{37}$ based on core-tops from the eastern South Atlantic and the global ocean (60°N–0°S), *Geochim. Cosmochim. Acta*, *62*, 1757–1772, doi:10.1016/S0016-7037(98)00097-0.

Müller, U. C., and J. Pross (2007), Lessons from the past: Present insolation minimum holds potential for glacial inception, *Quat. Sci. Rev.*, *26*, 3025–3029, doi:10.1016/j.quascirev.2007.10.006.

Oppo, D. W., J. F. McManus, and J. L. Cullen (1998), Abrupt climate events 500,000 to 340,000 years ago: Evidence from subpolar North Atlantic sediments, *Science*, *279*, 1335–1338, doi:10.1126/science.279.5355.1335.

Ortiz, J. T., A. C. Mix, and R. W. Collier (1995), Environmental control of living symbiotic and asymbiotic foraminifera of the California Current, *Paleoceanography*, *10*, 987–1009, doi:10.1029/95PA02088.

Peeters, F. J. C. (2008), Is the Indian Ocean a heat source for late Pleistocene deglaciations?, *Geophys. Res. Abstr.*, *10*, Abstract EGU2008-A-08923.

Peeters, F. J. C., R. Acheson, G.-J. A. Brummer, W. P. M. de Ruijter, R. R. Schneider, G. M. Ganssen, E. Ufkes, and D. Kroon (2004), Vigorous exchange between the Indian and Atlantic oceans at the end of the past five glacial periods, *Nature*, *430*, 661–665, doi:10.1038/nature02785.

Pierre, C., J. F. Saliege, M. J. Urrutiaguer, and J. Giradeau (2001), Stable isotope record of the last 500 k.y. at Site 1087 (southern Cape Basin), *Proc. Ocean Drill. Program Sci. Results*, *175*, 1–22.

Prahl, F. G., and S. G. Wakeham (1987), Calibration of unsaturation patterns in long-chain ketone compositions for palaeotemperature assessment, *Nature*, *330*, 367–369, doi:10.1038/330367a0.

Rau, A. J., J. Rogers, J. R. E. Lutjeharms, J. Giraudeau, J. A. Lee-Thorpe, M.-T. Chen, and C. Waelbroeck (2002), A 450-kyr record of hydrological conditions on the western Agulhas bank slope, south of Africa, *Mar. Geol.*, *180*, 183–201, doi:10.1016/S0025-3227(01)00213-4.

Rau, A. J., J. Rogers, and M.-T. Chen (2006), Late Quaternary paleoceanographic record in giant piston cores off South Africa, possibly including evidence of neotectonism, *Quat. Int.*, *148*, 65–77, doi:10.1016/j.quaint.2005.11.007.

Rohling, E. J. (2000), Paleosalinity: Confidence limits and future applications, *Mar. Geol.*, *163*, 1–11, doi:10.1016/S0025-3227(99)00097-3.

Rohling, E. J., K. Grant, M. Bolshaw, A. P. Roberts, M. Siddall, C. Hemleben, and M. Kucera (2009), Antarctic temperature and global sea level closely coupled over the past five glacial cycles, *Nat. Geosci.*, *2*, 500–504, doi:10.1038/ngeo557.

Romero, O., B. Boeckel, B. Donner, G. Lavik, G. Fischer, and G. Wefer (2002), Seasonal productivity dynamics in the pelagic central Benguela system inferred from the flux of carbonate and silicate organisms, *J. Mar. Syst.*, *37*, 259–278, doi:10.1016/S0924-7963(02)00189-6.

Rühlemann, C., S. Multiza, P. J. Muller, G. Wefer, and R. Zahn (1999), Warming of the tropical Atlantic Ocean and slowdown of the thermohaline circulation during the last deglaciation, *Nature*, *402*, 511–514, doi:10.1038/990069.

Rühlemann, C., S. Mulitza, G. Lohmann, A. Paul, M. Prange, and G. Wefer (2004), Intermediate depth warming in the tropical Atlantic related to weakened thermohaline circulation: Combining paleoclimate data and modeling results for the last deglaciation, *Paleoceanography*, *19*, PA1025, doi:10.1029/2003PA000948.

Sachs, J. P., R. F. Anderson, and S. J. Lehman (2001), Glacial surface temperatures of the southeast Atlantic Ocean, *Science*, *293*, 2077–2079, doi:10.1126/science.1063584.

Saunders, P. M., and B. A. King (1995), Oceanic fluxes on the WOCE A11 section, *J. Phys. Oceanogr.*, *25*, 1942–1958, doi:10.1175/1520-0485(1995)025<1942:OFOTWA>2.0.CO;2.

Schmidt, G. A., G. R. Bigg, and E. J. Rohling (1999), Global Seawater Oxygen-18 Database, http://data.giss.nasa.gov/o18data/, Goddard Inst. for Space Stud., New York.

Schmidt, M. W., M. J. Vautravers, and H. J. Spero (2006), Western Caribbean sea surface temperatures during the late Quaternary, *Geochem. Geophys. Geosyst.*, *7*, Q02P10, doi:10.1029/2005GC000957.

Schneider, R. R., P. J. Muller, and G. Ruhland (1995), Late Quaternary surface circulation in the east equatorial South Atlantic: Evidence from alkenone sea surface temperatures, *Paleoceanography*, *10*, 197–219, doi:10.1029/94PA03308.

Shannon, L. V., and G. Nelson (1996), The Benguela: Large scale features and processes and system variability, in *The South Atlantic: Present and Past Circulation*, edited by G. Wefer et al., pp. 163–210, Springer, Berlin.

Siedler, G., T. J. Muller, R. Onken, M. Arhan, H. Mercier, B. A. King, and P. M. Saunders (1996), The zonal WOCE sections in the South Atlantic, in *The South Atlantic: Past and Present Circulation*, edited by G. Wefer et al., pp. 83–104, Springer, Berlin.

Spero, H. J., J. Bijima, D. W. Lea, and B. E. Bemis (1997), Effect of seawater carbonate concentration on foraminiferal carbon and oxygen isotopes, *Nature*, *390*, 497–500, doi:10.1038/37333.

Stramma, L., and R. G. Peterson (1990), The South Atlantic Current, *J. Phys. Oceanogr.*, *20*, 846–859, doi:10.1175/1520-0485(1990)020<0846:TSAC>2.0.CO;2.

Thierstein, H. R., K. R. Geitzenauer, B. Molfino, and N. J. Shackleton (1977), Global synchroneity of late Quaternary coccolith datum levels: Validation by oxygen isotopes, *Geology*, *5*, 400–404, doi:10.1130/0091-7613(1977)5<400:GSOLQC>2.0.CO;2.

Wefer, G., et al. (1996), Late Quaternary surface circulation in the South Atlantic: The stable isotope record and implications for ocean heat transport and productivity, in *The South Atlantic: Present and Past Circulation*, edited by G. Wefer et al., pp. 461–502, Springer, Berlin.

Weijer, W., W. P. M. De Ruijter, A. Sterl, and S. S. Drijhout (2002), Response of the Atlantic overturning circulation to South Atlantic sources of buoyancy, *Global Planet. Change*, *34*, 293–311, doi:10.1016/S0921-8181(02)00121-2.

Westerhold, T. (2003), The middle-Miocene carbonate crash: Relationship to Neogene changes in ocean circulation and global climate, Ph.D. thesis, Univ. of Bremen, Bremen, Germany.

Zahn, R. (2009), Climate change: Beyond the CO_2 connection, *Nature*, *460*, 335–336, doi:10.1038/460335a.

Ziveri, P., H. Stoll, I. Probert, C. Klaas, M. Geisen, G. Ganssen, and J. Young (2003), Stable isotope 'vital effects' in coccolith calcite, *Earth Planet. Sci. Lett.*, *210*, 137–149, doi:10.1016/S0012-821X(03)00101-8.

J. A. Bendle, Glasgow Molecular Organic Geochemical Laboratory, Department of Geographical and Earth Sciences, University of Glasgow, Gregory Bldg., Lilybank Gdns., Glasgow G12 8QQ, UK.

A. J. Dickson, Department of Earth and Environmental Sciences, Open University, Milton Keynes MK7 6AA, UK. (a.j.dickson@dunelm.org.uk)

J. Green, M. J. Leng, and H. J. Sloane, NERC Isotope Geosciences Laboratory, British Geological Survey, Keyworth, Nottingham NG12 5GG, UK.

M. A. Maslin, Department of Geography, Environmental Change Research Centre, University College London, Pearson Bldg., Gower St., London WC1E 6BT, UK.

E. L. McClymont, School of Geography, Politics, and Sociology, University of Newcastle upon Tyne, Newcastle upon Tyne NE1 7RU, UK.

R. D. Pancost, Organic Geochemistry Unit, Bristol Biogeochemistry Research Centre, School of Chemistry, University of Bristol, Bristol BS8 1TS, UK.